

## Monte Carlo event generators & the top quark forward–backward asymmetry

Jan Winter<sup>1,2,a</sup>, Peter Z. Skands<sup>2,b</sup>, and Bryan R. Webber<sup>3,c</sup>

<sup>1</sup>Max-Planck-Institute for Physics, Föhringer Ring 6, D-80805 Munich, Germany

<sup>2</sup>PH-TH Department, CERN, CH-1211 Geneva 23, Switzerland

<sup>3</sup>Cavendish Laboratory, University of Cambridge, JJ Thomson Avenue, Cambridge CB3 0HE, UK

**Abstract.** The leading-order accurate description of  $t\bar{t}$  production, as usually employed in standard Monte Carlo event generators, gives no rise to the generation of a forward–backward asymmetry,  $A_{FB}$ . Yet, non-negligible – differential as well as inclusive – asymmetries may be produced if coherent parton showering is used in the hadroproduction of top quark pairs. In this contribution we summarize the outcome of our study [1] of this effect. We present a short comparison of different parton shower implementations and briefly comment on the phenomenology of the colour coherence effect at the Tevatron.

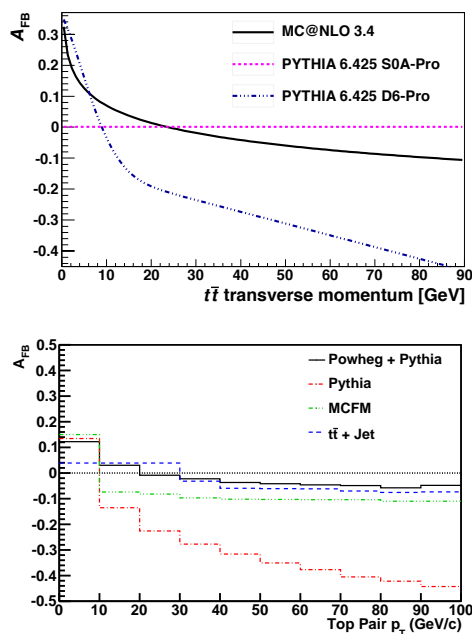


**Figure 1.** The top quark forward–backward asymmetry  $A_{FB}$  in dependence on the transverse momentum of the pair. Results from MC@NLO [2], PYTHIA [3], POWHEG [4], MCFM [5] and  $t\bar{t}$ +jet production at NLO [6] are shown as reported by the DØ and CDF collaborations in Refs. [7] and [8], respectively.

### 1 Introduction

In a number of different measurements the Tevatron collaborations both CDF and DØ reported results on the top quark forward–backward asymmetry that clearly lie be-

yond the Standard Model expectations for this quantity, see Refs. [7–10]. They did not only determine inclusive asymmetries but presented also differential distributions, such as  $A_{FB}(m_{t\bar{t}})$ , showing the asymmetry in different bins of observables  $O$  that reflect the kinematic properties of the reconstructed top quark system. One such observable is the transverse momentum of the pair,  $p_{T,t\bar{t}}$ , for which DØ made an interesting observation, documented in Ref. [7], while studying various Monte Carlo (MC) predictions: the leading-order (LO) event generator PYTHIA [3], using the option for approximate angular coherence, displays a qualitatively similar  $p_{T,t\bar{t}}$  dependent asymmetry to that of the next-to LO (NLO) matched parton shower, MC@NLO [2]; cf. the top panel in figure 1. Disabling the coherent shower option will restore the expected behaviour for PYTHIA as indicated by the dashed line (magenta) in the figure. CDF later on published similar results [8] confirming DØ’s observation; this is also shown in figure 1, at the bottom.

The definition of  $A_{FB}$  used by the Tevatron experimentalists is based on taking the rapidity difference between the top and the antitop quark,  $\Delta y = y_t - y_{\bar{t}}$ , and dividing the events according to their  $\Delta y$  hemisphere:

$$A_{FB}(O) = \frac{\left(\frac{d\sigma}{dO}\right)_+ - \left(\frac{d\sigma}{dO}\right)_-}{\left(\frac{d\sigma}{dO}\right)_+ + \left(\frac{d\sigma}{dO}\right)_-}. \quad (1)$$

The terms  $(d\sigma/dO)_\pm$  denote the differential (or, if  $O \equiv \mathbb{1}$ , inclusive) cross sections measured for forward/backward ( $\pm\Delta y > 0$ ) top quark pair configurations; note that  $\Delta y$  is a longitudinally boost invariant quantity. We shall now investigate the effects of colour coherent parton showering on  $A_{FB}$  in more detail.

### 2 The QCD colour coherence effect

We can gain a qualitative understanding by considering the large- $N_C$  colour flows in the leading-order partonic

<sup>a</sup>e-mail: jan.winter@cern.ch

<sup>b</sup>e-mail: peter.skands@cern.ch

<sup>c</sup>e-mail: webber@hep.phy.cam.ac.uk

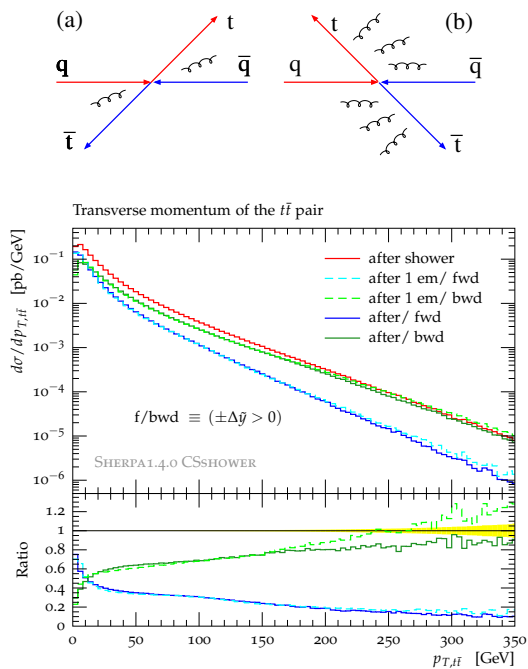


**Figure 2.** (Top) Colour flow and QCD radiation in (a) forward and (b) backward top quark pair production. (Bottom) SHERPA CSsHOWER [11, 12] predictions for all and separately generated forward/backward (fwd/bwd)  $t\bar{t}$  configurations at LO. The colour coherence effect is illustrated after the first and finally all shower emissions have occurred by means of the  $p_{T,\bar{t}t}$  distribution.

$q\bar{q} \rightarrow t\bar{t}$  processes, the by far dominant contributions to  $t\bar{t}$  production at the Tevatron. The (leading-)colour flows associated with these partonic interactions stretch from the initial to the final state connecting the incoming (anti)quark with the outgoing (anti)top quark. They form initial-final colour dipoles as shown in the upper part of figure 2. The deflection of the top quark out of the incoming quark's direction is a measure of the acceleration of the colour charge. Colour coherence manifests itself through this deflection angle: a mild scatter characterized by a small opening angle, keeping the forward motion of the top quark, only induces weak radiation off this  $qt$  dipole, see figure 2 upper left. In contrast, strong scattering and redirection of the top quark leads to a more violent acceleration of colour and hence a larger number of potentially also harder QCD emissions. Top quark pairs in backward configurations therefore experience an increased recoil which we illustrate in the upper right of figure 2. Consequently, we find a larger number of soft  $p_{T,\bar{t}t}$  events correlated with positive values of the asymmetry while hard  $p_{T,\bar{t}t}$  events often contribute to negative asymmetries – as well known from the NLO calculation, cf. figure 1.

We can easily test this rationale in a MC simulation which we do by utilizing SHERPA's CSsHOWER implementation [11].<sup>1</sup> We track the evolution of top quark pairs generated at leading, fixed order in forward ( $\Delta\tilde{y} > 0$ ) and backward ( $\Delta\tilde{y} < 0$ ) configurations independently.

<sup>1</sup>The use of dipole-like splitting kernels derived from spin-averaged, leading-colour reduced Catani–Seymour subtraction terms ensures an accurate treatment of the soft limit of QCD emission, thus, enables the construction of a colour coherent radiation pattern.

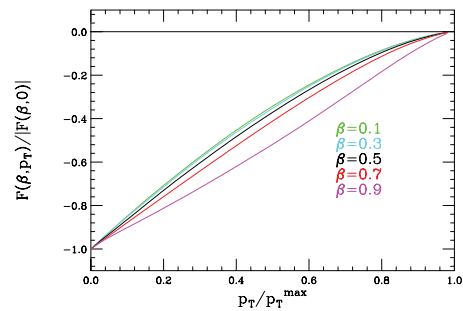


**Figure 3.** The function  $F(\beta, p_T)$ , normalized to its absolute value at zero  $p_T$ ; the maximum  $p_T$  is given as  $p_T^{\max} = \beta^2 \sqrt{\hat{s}}/2$ .

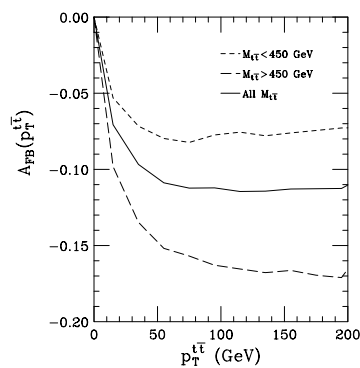


**Figure 4.** Leading-order QCD predictions (calculated with MCFM [5] at NLO in  $t\bar{t}$  production) for the forward–backward asymmetry as a function of  $p_T^{t\bar{t}}$  imposing an upper, a lower and no bound at all on the  $t\bar{t}$  pair mass.

The tilde sign in  $\Delta\tilde{y}$  is used to flag an evaluation at the matrix-element level. The results in the lower part of figure 2 clearly demonstrate that after the coherent showering phase, initial backward configurations yield a harder  $p_{T,\bar{t}t}$  spectrum than initially forwards moving top quark pairs. The latter preferably populate the soft region of  $p_{T,\bar{t}t} \lesssim 10$  GeV, and both observations thus agree well with our qualitative explanation from above.

## 2.1 Analytic approximation of the effect

The qualitative picture which we argued for in Sect. 2 can be made more explicit. Analyzing the real-emission contribution to the asymmetry, mainly arising from  $q\bar{q} \rightarrow t\bar{t}g$  processes, one can show, see Ref. [1], that the differential dependence of the asymmetry on the pair transverse momentum can be written as

$$\frac{p_T}{\hat{\sigma}_B} \frac{d\hat{\sigma}_A}{dp_T} = \frac{\alpha_s}{\pi} \frac{N_C^2 - 4}{N_C} F(\beta, p_T) \quad (2)$$

where  $p_T \equiv p_{T,\bar{t}t}$  and  $\beta = \sqrt{1 - 4m_t^2/\hat{s}}$  denotes the top quark center-of-mass velocity. The Born and asymmetry cross sections are given by  $\hat{\sigma}_B$  and  $\hat{\sigma}_A$ , respectively.

We can now discuss to what extent a coherent branching algorithm reproduces this functional form given in Eq. (2). Such shower generators treat the gluon radiation as coherent emission from the top quarks lines of the Born process, therefore overestimate the colour factor in Eq. (2) by  $2C_F = (N_C^2 - 1)/N_C$  (a 60% overestimate) and approximate the kinematic part of the asymmetry amplitude by the corresponding Born term times

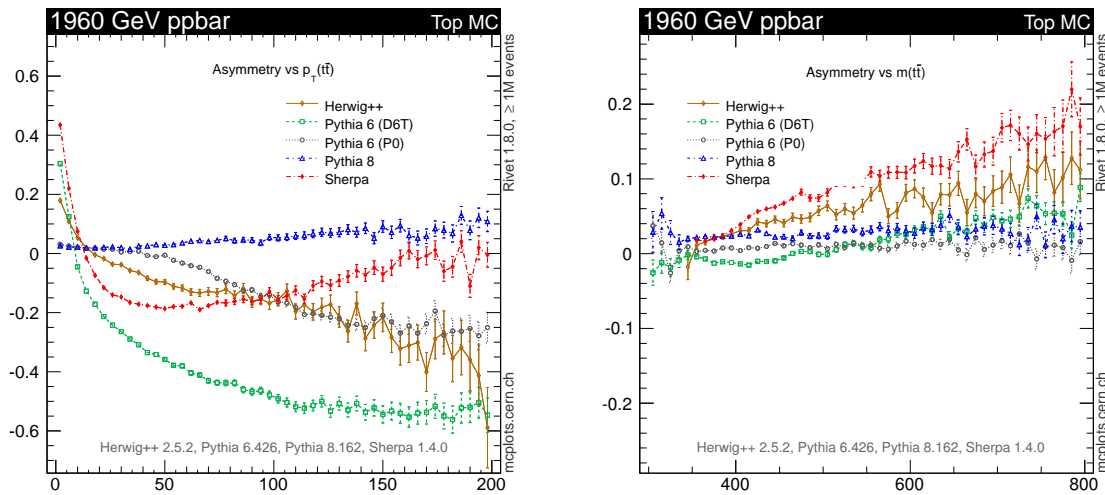


**Figure 5.** Differential asymmetries  $A_{FB}$  as a function of the pair transverse momentum ( $p_{T,t\bar{t}}$  in GeV, left panel) and  $t\bar{t}$  mass ( $m_{t\bar{t}}$  in GeV, right panel). Various predictions (and their MC errors) given by LO event generators are compared to each other.

dipole-like/eikonal factors. That means we effectively obtain a description of the asymmetry which is correct in the soft gluon limit (apart from the colour factor), but only approximate for  $p_T > 0$ , i.e. in the coherent shower generators the coupling- and colour-stripped asymmetry function  $F(\beta, p_T)$  given in Eq. (2) can only be “underestimated” by  $F(\beta, 0)$  which reads  $F(\beta, 0) = -4\beta - \beta^3 + \mathcal{O}(\beta^5)$  when Taylor expanded in  $\beta$ . Note that  $F(\beta, p_T)$  becomes less negative the further away from the  $p_T = 0$  limit. This is depicted in figure 3 for different fixed values of  $\beta$  where we observe larger deviations for increasing top quark pair invariant masses. Both the colour factor and kinematic approximations lead to a more pronounced  $A_{FB}(p_{T,t\bar{t}})$  dependence, as seen in figure 1 when comparing the PYTHIA coherent shower prediction with that given by MC@NLO.

Finally, figure 4 shows the  $p_T > 0$  dependence of the asymmetry as defined in Eq. (1) which one obtains from a full NLO calculation for  $t\bar{t}$  production at the Tevatron.<sup>2</sup> It is interesting to note that the asymmetry approaches zero but does not become positive as  $p_T \rightarrow 0$ . This is because the singularity structures present in the numerator and denominator are different. The denominator diverges faster owing to initial-state collinear singularities that cancel in the numerator. In contrast to the behaviour at fixed order, NLO matched or coherent parton showers predict an  $A_{FB}(p_{T,t\bar{t}})$  cross-over, as shown in figure 1, at low but non-negligible values of  $p_T$ . This is a consequence of the Sudakov suppression of small  $p_T$  occurring due to multiple soft gluon emission, an effect absent in the fixed-order description. This Sudakov suppression yields a spreading of the positive asymmetry over a finite region of  $p_T \gtrsim 0$ .

### 3 Differential asymmetry predictions

Considering the impact colour coherence has on generating differential asymmetries, it is important to study the

<sup>2</sup>The finite part of the virtual correction leads to a positive delta peak contribution at  $p_T \equiv 0$  which however is not shown here.

response of standard MC event generators using  $t\bar{t}$  production (without decays) at the Tevatron. For a representative collection of parton showers, we present their respective asymmetry predictions in figure 5 as functions of  $p_{T,t\bar{t}}$  (left panel) and  $m_{t\bar{t}}$  (right panel). Far more details regarding this MC tools comparison and the choice of parameters can be found in Ref. [1]. Here we only highlight a small fraction of the results of this comparison.

As one can see from figure 5, default HERWIG++ [13] and SHERPA [12] produce differential  $A_{FB}$  sufficiently similar to what one expects from the approximate NLO treatment mentioned above, especially the rise of  $A_{FB}$  with increasing  $m_{t\bar{t}}$  is remarkable. Using the  $m_{t\bar{t}}$  observable the Sudakov region is stretched/applied over the entire mass range which leads to a (an almost entirely) positive  $A_{FB}$  dependence. Both HERWIG++ (through angular ordering) and SHERPA (through dipole showering) have implemented QCD coherence in a proper way, however rely on different strategies regarding initial shower conditions and treatment of recoils. This induces differences between their predictions as seen in figure 5. While the version of PYTHIA 8 [14] used here does not yet account for QCD coherence effects, hence produces rather small,  $p_{T,t\bar{t}}$  as well as  $m_{t\bar{t}}$  insensitive asymmetries, the PYTHIA 6 [3] predictions in figure 5 are examples for the fact that the older generation provides options (tunes) with varying amount of coherence. The D6T and P(erugia)0 tunes [15] emerged from efforts to improve the description of Tevatron and LHC data, respectively. In particular the D6T tune amplifies the effect of colour coherence as explained in Ref. [1].

### 4 Inclusive asymmetry and longitudinal recoil effects

Inspecting the numbers in table 1, it is obvious that colour coherent showering not only produces non-trivial differen-

**Table 1.** Inclusive  $A_{\text{FB}}$  (in %) in each shower model, and to leading, non-trivial order in QCD (taken from  $\text{MCFM}$ ).

Model	Version	$A_{\text{FB}}$	Model	Version	$A_{\text{FB}}$
PYTHIA 6	6.426	-0.1	SHERPA	1.4.0	5.5
PYTHIA 8	8.163	2.5	QCD	LO	6.0
HERWIG++	2.5.2	3.9			

tial asymmetries but also an inclusive  $A_{\text{FB}}$ .<sup>3</sup> This clearly comes as another surprise, but can be explained via event migrations arising from longitudinal recoil effects. This is specified in Ref. [1] where we also show that the effect, already at LO, may give a relevant contribution to the inclusive asymmetry. Here, we only want to provide evidence that migration indeed occurs in coherent showers, using the  $\text{CSHOWER}$  results displayed in figure 6.

Following the same strategy used to produce the  $p_{T,\bar{t}\bar{t}}$  spectra presented in figure 2, it is straightforward to obtain the corresponding  $\Delta y$  distributions to examine the migration effect directly. A simple visualization of the longitudinal recoil effect comes in terms of a stretching/widening of the gluon emitting  $qt$  initial-final dipole. Independently of the magnitude of the initial scattering angle, the top quark will be slightly pushed forward while the antitop quark retains its direction such that  $\Delta y = \Delta\tilde{y} + \epsilon$  is a plausible parametrization ( $\epsilon > 0$ ). The results shown in figure 6 confirm this conjecture. Several observations are made: (1) the imbalance between  $\Delta y < 0$  and  $\Delta y > 0$  events, i.e. the generated asymmetry, is clearly visible by comparing the after- with the before-shower result (cf. red vs. black line), (2) the migration of initial backward and forward configurations to higher values of  $\Delta y$  produces an overflow of events of the former category closing the dip at  $\Delta y \gtrsim 0$  generated by shifted events of the latter category (cf. green vs. blue lines), (3)  $+ \rightarrow -$  migrations in  $\Delta y$  (i.e.  $\epsilon < 0$ ) are suppressed and (4) the largest contribution to the migration effect already appears with the first emission (cf. dashed vs. solid lines). Generally, migrations are small, occur locally and clearly favour  $\epsilon > 0$ . They therefore fuel the generation of a positive-valued inclusive asymmetry.

## 5 Phenomenological tests

With our understanding of the origin of the colour coherence effect, we can study some of its phenomenological implications which we briefly discuss below.

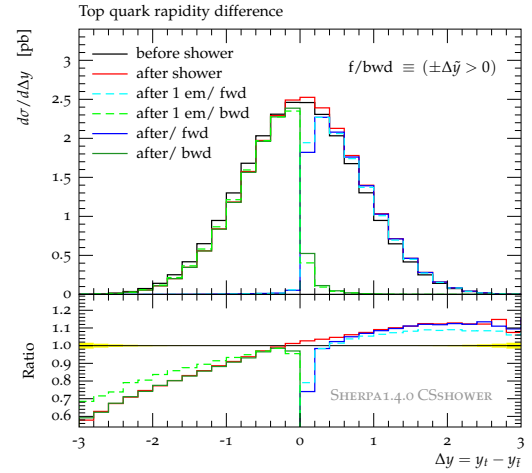
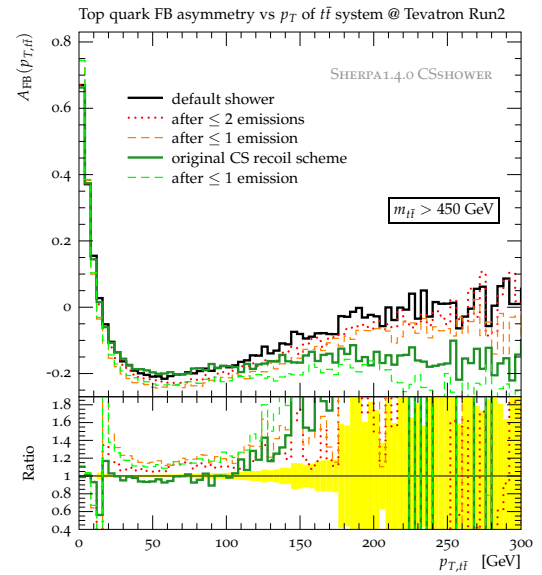
### 5.1 Asymmetry in different phase-space domains

By focusing on certain phase-space regions, one can amplify the inclusive asymmetry, as shown in table 2. The application of cuts isolating large  $m_{\bar{t}\bar{t}}$  or low  $p_{T,\bar{t}\bar{t}}$  leads to an increase of the positive asymmetry. The latter cut is particularly useful to efficiently separate off the Sudakov region, i.e. the domain of low  $p_{T,\bar{t}\bar{t}}$  that generates the positive contribution to the overall asymmetry. Considering

<sup>3</sup>This can also be anticipated by viewing  $\text{HERWIG++}$ 's and  $\text{SHERPA}$ 's positive-valued  $A_{\text{FB}}(m_{\bar{t}\bar{t}})$  results given in figure 5.

**Table 2.** Inclusive  $A_{\text{FB}}$  results (in %) imposing simple kinematic cuts ( $M = 450$  GeV,  $Q = 50$  GeV) for the  $\text{HERWIG++}$  model, the  $\text{CSHOWER}$  and  $\bar{t}\bar{t}$  production at NLO (computed with  $\text{MCFM}$ ).

Model	Version	$m_{\bar{t}\bar{t}} < M$	$> M$	$p_{T,\bar{t}\bar{t}} < Q$	$> Q$
$\text{HERWIG++}$	2.5.2	2.7	6.0	5.8	-14.3
$\text{SHERPA}$	1.4.0	3.5	9.2	8.7	-15.4
QCD	LO	4.1	9.3	7.0	-11.1

**Figure 6.** The  $\Delta y$  distributions for various modes of  $\text{CSHOWER}$  applied after disjoined as well as joined  $\Delta\tilde{y}$  hemisphere generation at leading, fixed order in top quark pair production.**Figure 7.**  $A_{\text{FB}}(p_{T,\bar{t}\bar{t}})$  distributions obtained after coherent parton showering (computed with the  $\text{CSHOWER}$  [11]) for the constraint of large pair masses,  $m_{\bar{t}\bar{t}} > 450$  GeV. The brighter dashed/dotted curves indicate the impact of the first two emissions. The green solid curve shows the outcome of a recoil scheme variation (as provided by  $\text{SHERPA}$  v.1.4.0 [12]).

the anti-cut (real-emission) region, one can test the most striking feature of the transition in  $p_{T,\bar{t}\bar{t}}$  domains: that is the sign change in the asymmetry. Because of the approximations discussed earlier, coherent showers predict a stronger

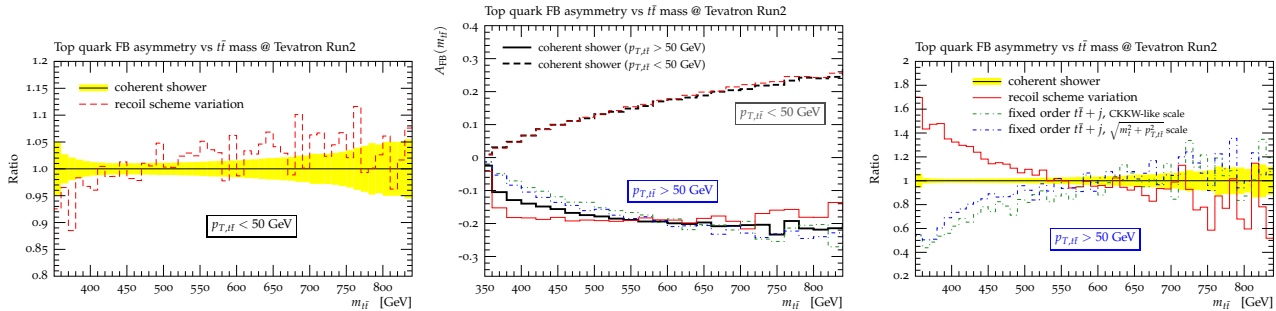


**Figure 8.**  $A_{\text{FB}}(m_{t\bar{t}})$  predictions (center) and ratio plots using colour coherent showering (here computed by SHERPA’s CSSHOWER [11]) for a  $p_{T,t\bar{t}}$  domain separation at  $p_{T,t\bar{t}} = 50$  GeV. A recoil scheme variation (as provided by SHERPA v.1.4.0) is also shown as well as reference curves for lowest-order  $t\bar{t}j$  production employing different scale choices.

asymmetry flip at large  $p_{T,t\bar{t}}$ . For all other cases, they however give enhancements similar to the NLO result.

These single-cut,  $A_{\text{FB}}$  enhancing effects can also be found at the differential level. We exemplify this in figures 7 and 8 using SHERPA CSSHOWER results. Figure 8 is shown to compare the different  $A_{\text{FB}}(m_{t\bar{t}})$  distributions associated with the two  $p_{T,t\bar{t}}$  domains. It exhibits the sign flip in the asymmetry very clearly. The opposite scenario is presented in Figure 7 where small top quark pair masses are vetoed and  $A_{\text{FB}}$  is shown as a function of the pair transverse momentum. As expected, the increase of  $A_{\text{FB}}$  is most noticeable in the first few  $p_{T,t\bar{t}}$  bins, those that are close to zero. In both figures we also illustrate the impact of a recoil scheme variation (as provided by SHERPA v.1.4.0): differences only occur in the high  $p_{T,t\bar{t}}$  region where the amount of Tevatron data is too sparse to discriminate between the two options.

## 5.2 Top quark velocity dependence of the asymmetry

We want to briefly discuss how the coherence effect (generating non-zero  $A_{\text{FB}}$ ) changes under variation of the top quark mass and collider energy  $\sqrt{s}$ . It is thus convenient to analyze the  $\beta$  dependence of the asymmetry, which behaves roughly like  $A_{\text{FB}}(m_{t\bar{t}})$ . Figure 9 contains a number of  $A_{\text{FB}}(\beta)$  curves obtained from coherent showering using different values for the  $m$  and  $s$  parameters. Apart from PDF effects, one finds, as expected, an approximately stable asymmetry dependence, if mass and  $\sqrt{s}$  are scaled equally. Investigating the limiting cases, it is clear that the dramatic increase of  $A_{\text{FB}}$  occurs as a consequence of reaching the collider phase-space boundaries. The contribution to the inclusive asymmetry however is small since the cross section of the associated phase-space area is tiny.

## 5.3 Top quark forward–backward asymmetry from the lepton perspective

We gain information if we define the analysis not only in terms of the forward–backward asymmetry,  $A_{t\bar{t}} \equiv A_{\text{FB}}$ , but also in terms of a lepton-based asymmetry  $A_l$  (now including top quark decays). This allows one to exploit the way

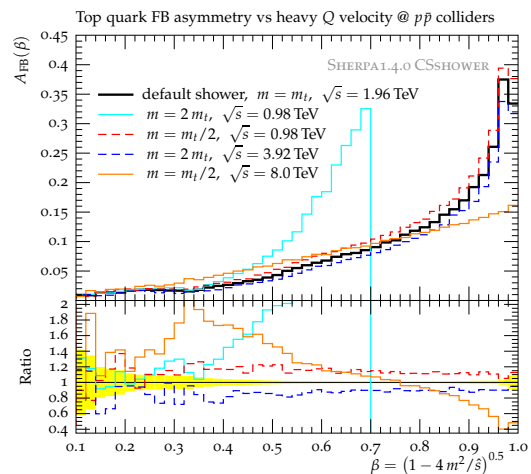


**Figure 9.**  $A_{\text{FB}}(\beta)$  distributions obtained from coherent parton showering (as implemented in the CSSHOWER [11]) for varying “top quark” masses,  $m$ , and  $p\bar{p}$  collider energies,  $\sqrt{s}$ .

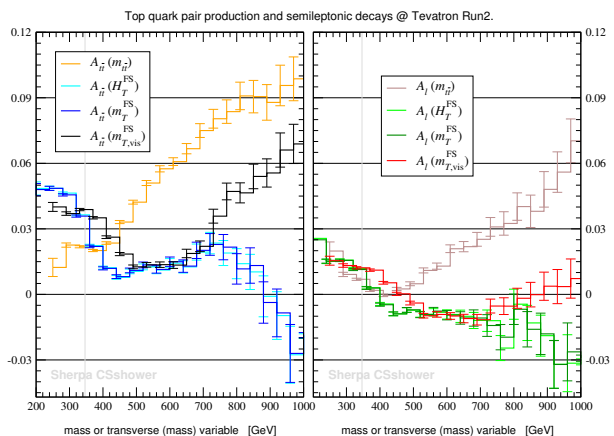


**Figure 10.** Differential forward–backward ( $A_{t\bar{t}} \equiv A_{\text{FB}}$ ) and lepton-based ( $A_l$ ) asymmetries given in terms of various (transverse) mass observables [16]. Here, CSSHOWER results are shown.

these asymmetries are correlated in the Standard Model and beyond; for the details see Ref. [16]. An example for coherent shower predictions in terms of (transverse) mass observables, see also [17], is given in figure 10 relat-

ing results for reconstructed top quarks ( $A_{t\bar{t}}$ ,  $A_{t\bar{t}}(m_{t\bar{t}})$ , etc.) with results where this reconstruction is not ( $A_l$ ,  $A_l(m_{T,\text{vis}}^{\text{FS}})$ , etc.) or only partially ( $A_{t\bar{t}}(H_T^{\text{FS}})$ ,  $A_l(m_{t\bar{t}})$ , etc.) required (the “ $O^{\text{FS}}$ ” superscript signifies that the transverse observables used here are obtained from all final-state visible objects and  $\cancel{E}_T$ ). This introduces additional analysis handles and levels, and therefore more directions to cross-check the data for consistency or potential biases.

## 6 Summary

Even in the absence of a full NLO treatment, standard Monte Carlo event generators can produce significant differential as well as inclusive forward–backward asymmetries in top quark pair production. These asymmetries arise from valid physics built into generators relying on (approximately) coherent parton or dipole showering. While colour coherent shower algorithms cannot be quantitatively correct in every detail, they are able to capture important features as known from QCD higher-order calculations. Based on these findings, coherent showers are qualified to serve as fast tools in estimating the Standard Model phenomenology of the forward–backward asymmetry.<sup>4</sup> However, if used in data analyses to determine Monte Carlo corrections, one needs to be aware of their previously unexpected asymmetry-generating behaviour.

## Acknowledgments

J.W. would like to thank the organizers and conveners of the HCP2012 symposium for arranging a fantastic conference. Additionally, financial support by the local organizing committee is gratefully acknowledged.

<sup>4</sup>For a recent example, see Ref. [16], where coherent shower predictions are used to estimate the correlation between  $A_{t\bar{t}} \equiv A_{\text{FB}}$  and  $A_l$ , the lepton-based asymmetry definable in the semileptonic decay channel.

## References

- [1] P.Z. Skands, B.R. Webber, J. Winter, JHEP **1207**, 151 (2012), 1205.1466
- [2] S. Frixione, P. Nason, B.R. Webber, JHEP **0308**, 007 (2003), hep-ph/0305252
- [3] T. Sjöstrand, S. Mrenna, P.Z. Skands, JHEP **0605**, 026 (2006), hep-ph/0603175
- [4] S. Frixione, P. Nason, G. Ridolfi, JHEP **0709**, 126 (2007), 0707.3088
- [5] J.M. Campbell, R.K. Ellis (2012), 1204.1513
- [6] K. Melnikov, A. Scharf, M. Schulze, Phys.Rev. **D85**, 054002 (2012), 1111.4991
- [7] V.M. Abazov et al. (DØ Collaboration), Phys.Rev. **D84**, 112005 (2011), 1107.4995
- [8] T. Aaltonen et al. (CDF Collaboration) (2012), 1211.1003
- [9] T. Aaltonen et al. (CDF Collaboration), Phys.Rev. **D83**, 112003 (2011), 1101.0034
- [10] V.M. Abazov et al. (DØ Collaboration) (2012), 1207.0364
- [11] S. Schumann, F. Krauss, JHEP **0803**, 038 (2008), 0709.1027
- [12] T. Gleisberg, S. Höche, F. Krauss, M. Schönherr, S. Schumann et al., JHEP **0902**, 007 (2009), 0811.4622
- [13] M. Bähr, S. Gieseke, M. Gigg, D. Grellscheid, K. Hamilton et al., Eur.Phys.J. **C58**, 639 (2008), 0803.0883
- [14] T. Sjöstrand, S. Mrenna, P.Z. Skands, Comput.Phys.Commun. **178**, 852 (2008), 0710.3820
- [15] P.Z. Skands, Phys.Rev. **D82**, 074018 (2010), 1005.3457
- [16] A. Falkowski, M.L. Mangano, A. Martin, G. Perez, J. Winter (2012), 1212.4003
- [17] J.D. Lykken, A. Martin, J. Winter, JHEP **1208**, 062 (2012), 1111.2881